Study of Microstructure and Mechanical Properties of Friction Stir Welded Ferrite-Martensite DP700 Steel

Mahdi Mahmoudiniya[1, 2, *], Leo A.I. Kestens[2, 3], Shahram Kheirandish[1], Amir Hossein Kokabi[4]

[1]*School of Metallurgy and Materials Engineering, Iran University of Science and Technology (IUST), Tehran, 16846-13114, Iran*
[2]*Department of Materials Science and Engineering, Delft University of Technology, Mekelweg 2, Delft, 2628 CD, the Netherlands*
[3]*Metals Science and Technology Group, Ghent University, Ghent, Technologiepark 903 B-9052 Zwijnaarde, Belgium*
[4]*Department of Materials Science and Engineering, Sharif University of Technology, Tehran, 11365-11155, Iran*

*Corresponding author: Fax: (+98) 9378545631; E-mail: mmahmoudiniya@metaleng.iust.ac.ir

Received: 12 August 2018, Revised: 18 September 2018 and Accepted: 26 October 2018

DOI: 10.5185/amlett.2019.2211
www.vbripress.com/aml

Abstract

In the present study, a 2 mm thick ferrite-martensite dual phase steel was subjected to friction stir welding. The welding was conducted by a tungsten carbide tool at a constant rotational speed of 800 rpm and various feed rates of 50, 100 and 150 mm/min. The microstructural features of friction stir welded joints were characterized by field emission - scanning electron microscopy as well as by transmission electron microscopy. The relationship between microstructure and tensile properties of the joints was investigated. Results showed that the stir zone of the welds consisted of bainite packets, exhibiting a different morphology compared to the ferrite phase and to the martensite phase. Microstructural examination of the heat affected zone showed that there is a softened region in the heat affected zone in all joints, irrespective of the welding speed. Decomposition of the martensite phase during tempering of the initial martensite of the base material was responsible for the observed hardness reduction. The decrease of the hardness in the softened zone was 28 ± 3, 21 ± 2.5 and 15 ± 3.2 HV for welding speeds of 50, 100 and 150 mm/min, respectively; whereby the base material exhibited a hardness of 275 ± 3 HV. The lower softening corresponded to the higher welding speed, i.e., under conditions whereby heat input to the weld was minimum. The tensile test results showed that the ultimate tensile strength of all welded joints is lower than the base metal and failure takes place in the softened region of the joints. The increment of welding speed increased the strength of the joint so that the weld conducted at the highest welding speed (150 mm/min) showed the highest tensile strength of 687 MPa, i.e. 95% of the strength of the base metal (723 MPa).

Keywords: Friction stir welding; ferrite-martensite dual phase steel; mechanical properties; microstructure

Introduction

Nowadays, the application of friction stir welding (FSW) has been significantly increased. Friction stir welding, as a solid-state welding technique, has some advantages over fusion welding techniques such as 1) avoiding some common defects that usually form during solidification in fusion welding processes, e.g. porosities and solidification cracks 2) lower distortion and residual stress because of the reduced heat input to the weld 3) friendly environmental process [**1, 2**]. These advantages have enabled FSW to be used for joining some materials that have serious issues during fusion welding.

Ferrite-martensite dual phase steels (DP), as a type of advanced high strength steels, are suffering from some issues accompanied by fusion welding techniques. An unavoidable issue during welding of DP steels is tempering of the initial martensite in the heat affected zone [**3, 4**]. Martensite, as a hard phase, is responsible for strengthening of DP steels while ferrite phase, as a soft phase, provides suitable ductility for the material [**5**].

Martensite, which can be regarded as a thermally unstable phase, decomposes during exposing to the heat, which is known as "tempering" [**6**]. In fact, the hard phase of martensite transforms into the ferrite and carbides as a result of tempering, which leads to the softening of HAZ [**4**]. The softened HAZ deteriorates the mechanical properties of the welded joint [**7, 8**]. Decreasing of heat input to the weld effectively will suppress HAZ softening phenomenon [**9**]. Since FSW is a solid-state joining technique, in which no melt form during the process, it is expected that heat input to the weld reduces significantly compared to the fusion welding techniques [**10**]. Accordingly, FSW can be regarded as an alternative welding method for joining of DP steels.

The present work, therefore, aimed to study microstructure and mechanical properties of the DP700 steel joints that have produced by friction stir welding.

Experimental

The material used for the present study was a DP700 steel sheet with a thickness of 2 mm. **Table 1** summarizes the chemical composition of DP700 steel sheet. The butt joint friction stir welding experiments were made using a FSW facility at a fixed rotational speed of 800 rpm and with different feed rates of 50, 100, 150 mm/min. A WC-Co material with a shoulder diameter of 16 mm, a pin diameter of 6 mm and a pin length of 1.8mm was used as FSW tool. An argon gas atmosphere was employed to minimize surface oxidation. The microstructure of the transverse section of the joints was characterized using optical microscopy, field emission scanning electron microscopy and transmission electron microscopy. The Vickers microhardness measurements were performed on the polished cross-sections under a load of 100 gr. Transverse tensile samples were cut using a wire cut machine according to ASTM-E8 [**11**]. The tensile tests were performed at a constant crosshead speed of 1mm/min.

Table 1. Chemical composition (%wt) of examined DP700 steel sheet.

C	Mn	Si	Ni	Cr	Cu
0.076	1.04	0.43	0.23	0.56	0.34

Results and discussions

The transverse macrostructure and microstructure of the welds are shown in **Figs. 1, 2** and **3**. The macrostructure of the joints reveals that sound welds, without any crack or channel defect, can be produced at welding speeds in the range of 50-150 mm/min.

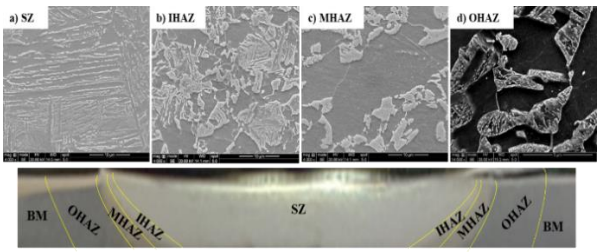

Fig. 1. Macrostructure and microstructure of the joint welded at the welding speed of 50 mm/min.

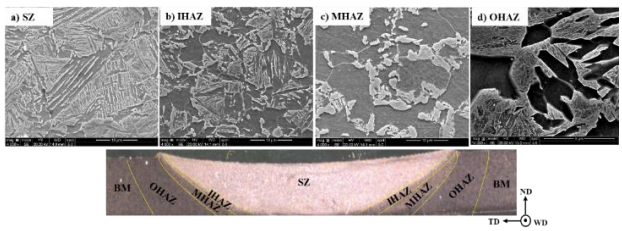

Fig. 2. Macrostructure and microstructure of the joint welded at the welding speed of 100 mm/min.

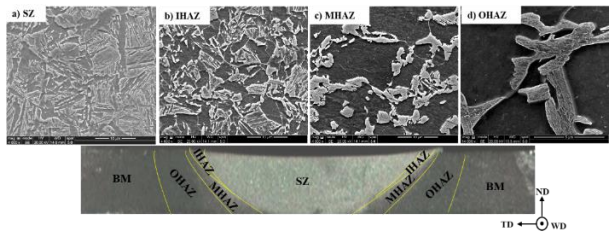

Fig. 3. Macrostructure and microstructure of the joint welded at the welding speed of 150 mm/min.

The macrostructure of the joints includes three different regions: base metal (BM), heat affected zone (HAZ) and the stir zone (SZ). The heat affected zone also can be subdivided to different zones include: inner HAZ (the first region of HAZ that is adjacent to the stir zone), outer HAZ (a part of HAZ that is adjacent to the base metal) and middle HAZ (the middle part of HAZ). The microstructure of each zone will be described in details.

Fig. 4 represents the microstructure of the base metal as observed by STEM and FE-SEM. DP700 steel consists of a ferrite matrix and 20% martensite. The STEM image, **Fig. 4b**, reveals that a large number of dislocations randomly have distributed in the ferrite phase.

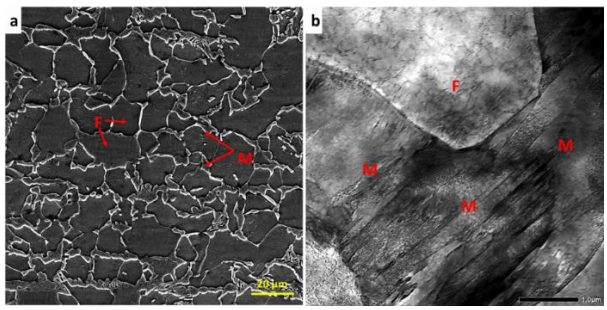

Fig. 4. Microstructure of the base metal a) SEM image b) STEM image (F: ferrite, M: martensite).

As can be seen (**Figs 1a, 2a** and **3a**), the stir zone of the joints predominantly consists of bainite packets, different morphologies of ferrite as well as martensite. Microstructural examination of the stir zone, which is a function of thermomechanical conditions during processing, exhibited that materials in the center of the stir zone for all welding speeds have experienced a peak temperature higher than Ac_3 before cooling. Generally, because of co-existence of heat and severe strain in the stir zone, dynamic recrystallization takes place in the stir zone [**12**]. Comparing **Fig. 1a** with **Figs 2a** and **3a** reveals that the coarsest microstructure of the stir zone corresponds to the weld made at the lowest welding speed (50 mm/min). Increasing the welding speed decreases the peak temperature, while the strain and strain rate increase in the stir zone [**13**]. Accordingly, welding at low welding speed provides more suitable conditions for the recrystallized austenite grains to growth before cooling, whereby a coarsened structure will obtain.

It was found that the microstructure of IHAZ (**Figs 1b, 2b** and **3b**) mainly contains polygonal ferrite, bainitic ferrite as well as M-A islands. The peak

temperature in this region is higher than Ac_3 during welding, whereby the initial microstructure of the base metal transforms into the austenite phase during heating. Since the peak temperature is slightly above Ac_3, the prior austenite grains have almost a fine structure before cooling [**14**]. The finest microstructure of IHAZ corresponds to the joint made at highest welding speed, in which the lowest heat input introduces to the weld.

As can be seen in **Figs 1c, 2c** and **3c**, MHAZ consists of polygonal ferrite and martensite. In MHAZ, the initial microstructure is heated to temperatures between Ac_1 and Ac_3, which results in co-existence of the austenite and ferrite phase, whereby the austenite phase transforms into martensite while the ferrite phase remains unchanged after cooling [**6**].

Comparing MHAZ at different welding speeds, **Figs 1c, 2c** and **3c**, shows that the highest volume fraction of martensite in MHAZ corresponds to the joint which has processed in welding speed of 50 mm/min. The volume fraction of martensite is proportional to the volume fraction of austenite phase in dual phase domain ($\alpha + \gamma$) before cooling [**15**]. Higher heat input to the weld leads to the formation of the higher fraction of austenite phase during the heating cycle, which transforms into the martensite after cooling.

Figs 1d, 2d and **3d** present the microstructure of OHAZ, which consists of ferrite as well as tempered martensite. Since in OHAZ peak temperature remains lower than Ac_1 temperature, pre-existing martensite tempers during welding. During tempering phenomenon, martensite lathes recover and carbides precipitate from the martensite [**16**]. Fine particles of carbides can be seen easily in tempered martensite. It is obvious that precipitated carbides in **Fig. 1d** and are relatively coarser than those of **Fig. 2d** and **3d**. This indicates to a higher degree of tempering at lower welding speed. STEM micrograph of OHAZ for welding speed of 50 mm/min, **Fig. 5**, also clearly depicted decomposition of the martensite and carbide precipitation (red arrows) within a lath of martensite in which the precipitated carbides have an elongated shape with a length of less than 100 nm.

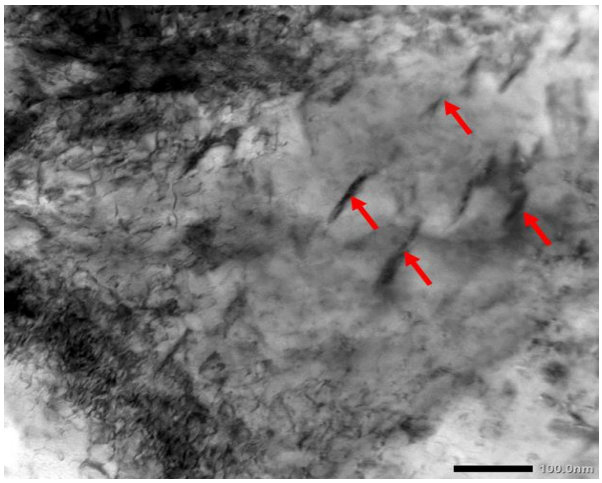

Fig. 5. STEM image of OHAZ processed at welding speed of 50 mm/min.

Fig. 6a presents the microhardness profile of the joints. The base metal exhibited an average hardness of 275±3 HV. While the stir zone exhibited the maximum microhardness, the minimum hardness of the joint corresponded to OHAZ. The higher hardness of the stir zone is attributed to the higher cooling rate at this region while tempering of martensite, which leads to the softening, is responsible for hardness reduction in OHAZ [17]. Joint processed at the welding speed of 50 mm/min exhibited higher hardness reduction in OHAZ (28±3 HV). This is attributed to the increase of the heat input with decreasing welding speed, which develops a higher degree of softening.

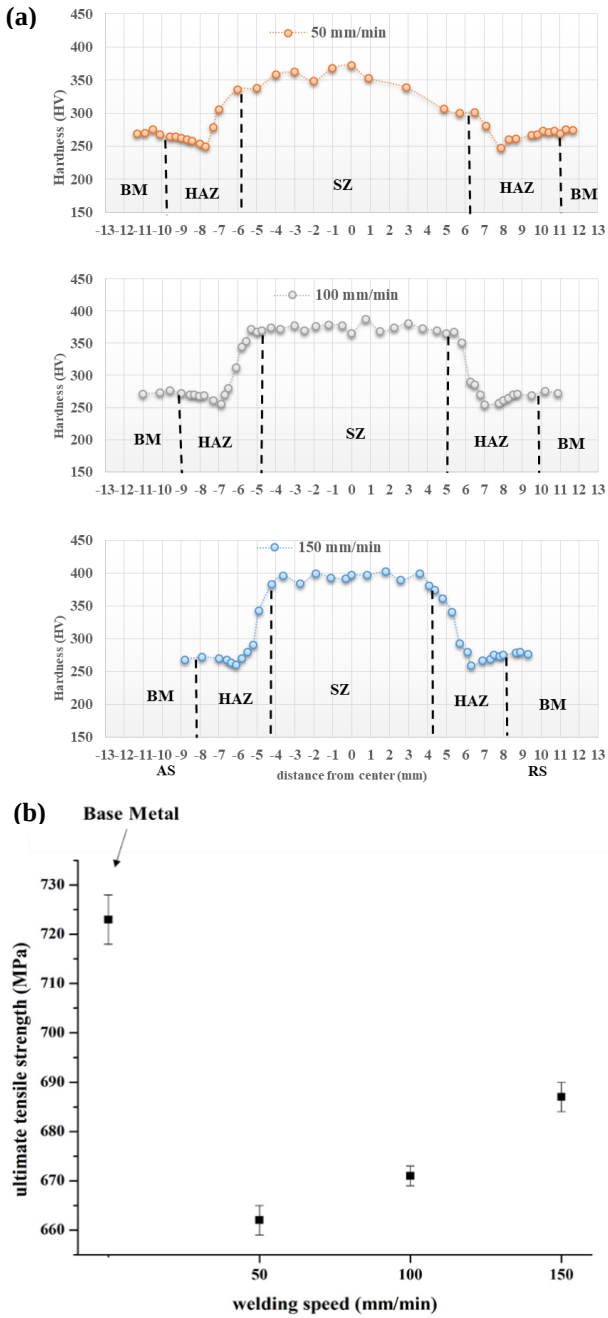

Fig. 6. (a) microhardness profiles in transverse section of the welds at different welding speeds (b) variation of UTS of welded samples with welding speed.

Fig. 6b shows some results of the transverse tensile tests of BM and the welded joints. It is also noticeable that BM sample failed at the center of gauge length while the welded tensile samples failed in OHAZ. The lowest hardness of the joints corresponds to OHAZ where the majority of the plastic strain accumulates during the tensile test and finally leads to the failure. Accordingly, the ultimate tensile strength of the welded joints is slightly lower than the base metal. Moreover, the highest ultimate tensile strength corresponds to the highest welding speed in which OHAZ has experienced the lowest hardness reduction.

Conclusion

In the present study, the effect of welding speed on the microstructure and mechanical properties of friction stir welded DP700 steel was investigated. The results showed that the sound and defect-free joints could be obtained at welding speeds of 50, 100 and 150 mm/min. The microstructure of the stir zone found to be a mixture of bainite, ferrite as well as martensite in all the joints. It also was found that the coarsest microstructure of the stir zone corresponds to the weld made at the lowest welding speed (50 mm/min). The microhardness results showed that the lowest hardness of the joints corresponds to OHAZ where the softening phenomenon was responsible for the reduction of the hardness compared to the base metal. All FSWed samples failed in the softened HAZ and showed lower strength and ductility in comparison with the base metal. The highest ultimate tensile strength of the joint corresponded to the highest welding speed in which OHAZ has experienced the lowest hardness reduction.

References

1. Nandan, R.; DebRoy, T.; Bhadeshia, H. K. D. H.; *Prog. Mater. Sci.*, **2008**, *53*, 980.
2. Mishra, R. S.; De, P. S.; Kumar, N.; Friction Stir Welding and Processing: Science and Engineering; Springer, **2014**.
3. Wang, J.; Yang, L.; Sun, M.; Liu, T.; Li, H.; *Mater. Des.*, **2016**, *90*, 642.
4. Cheng, G.; Zhang, F.; Ruimi, A.; Field, D. P.; Sun, X.; *Mater. Sci. Eng. A.*, **2016**, *667*, 240.
5. Galán, J.; Samek, L.; Verleysen, P.; Verbeken, K.; Houbaert, Y.; *Rev. Metal.*, **2012**, *48*, 118.
6. Wang, J.; Yang, L.; Sun, M.; Liu, T.;Li, H.; *Mater. Des.*, **2016**, *97*, 118.
7. Liu, Y.; Dong, D.; Wang, L.; Chu, X.; Wang, P.; Jin, M.; *Mater. Sci. Eng. A*, **2015**, *627*, 296.
8. Dong, D.; Liu, Y.; Yang, Y.; Li, J.; Ma, M.; Jiang, T.; *Mater. Sci. Eng. A*, **2014**, *594*, 17.
9. Xia, M.; Biro, E.; Tian, Z.; Zhou, Y. N.; *ISIJ Int.*, **2008**, *48*, 809.
10. Sarkar, R.; Pal, T. K.; Shome, M.; *Sci. Technol. Weld. Join.*, **2014**, *19*, 436.
11. ASTM Standard E 8: Standard test methods for tension testing of metallic materials, 03.01. ASTM, **2000**.
12. Lienert, T. J.; Stellwag Jr, W. L.; Grimmett, B. B.; Warke, R. W.; *Weld. J.*, **2003**, *82*, 1.
13. Husain, M. M.; Sarkar, R.; Pal, T. K.; Prabhu, N.; Ghosh, M.; *J. Mater. Eng. Perform.*, **2015**, *24*, 3673.
14. Jia, Q.; Guo, W.; Peng, P.; Li, M.; Zhu, Y.; Zou, G.; *J. Mater. Eng. Perform.*, **2016**, *25*, 668.
15. Bhadeshia, H. K. D. H.; Honeycombe, R.; Steels: Microstructure and Properties; Elsevier, **2011**.
16. Baltazar Hernandez, V. H.; Nayak, S. S.; Zhou, Y.; *Metall. Mater. Sci.*, **2011**, *42*, 3115.
17. Matsushita, M.; Kitani, Y.; Ikeda, R.; Ono, M.; Fujii, H.; Chung, Y. D.; *Sci. Technol. Weld. Join.*, **2011**, *16*, 181.

